Sensors and Materials, Vol. 36, No. 2 (2024) 403–413
MYU Tokyo

S & M 3527

Wireless Humidity Sensing with Chipless Radio Frequency Identification Tag

Bo Wang,* Junqiang He, Yalun Song, Ke Wang, and Shengli Cao

Xi'an University of Posts and Telecommunications, Xi'an, Shaanxi Province 710199, China

(Received October 2, 2023; accepted November 29, 2023)

Keywords: wireless humidity sensing, chipless RFID tag, moisture-sensitive film

In this study, a compact and flexible chipless radio frequency identification humidity sensor with dimensions of 21 × 21 mm^2 is realized. The resonator structure consists of a square open ring and a U-shaped ring on a Rogers TMM 4(tm) substrate. The Kapton relative permittivity is very sensitive to changes in ambient humidity, and the sensor is capable of detecting humidity when the resonator is covered with a Kapton film. The amplitude of the radar scattering cross section increases monotonically from −65.66 to −58.14 dB with an offset of 7.52 dB when the relative humidity (RH) increases from 40 to 90%. The chipless sensor designed in this study has a compact size of only 21 × 21 mm^2 with good resonance characteristics, and with the Kapton thin film covering, the sensor exhibits an excellent sensitivity of 0.15 dB/% RH. It also has a wide humidity measurement range from 40 to 90%.

1. Introduction

The Internet of Things (IoT) is an advanced information technology developing rapidly and significantly impacting several fields. It has already demonstrated great potential in our daily lives, social activities, manufacturing, and environmental protection. Radio frequency identification (RFID) is an indispensable technology in IoT, and microsensors are playing an increasingly critical role in modern society and are widely used in smart manufacturing, smart homes, disaster monitoring, and so forth.

The RFID system generally includes three core parts: computer, tag, and reading device. The working principle of the system is shown in Fig. 1. The reader transmits the inquiry signal to activate the tag, then the tag reflects back the echo signal towards the reader. The echo signal is decoded by the reader and processed by the computer. The computer integrates the data decoded from the echo signal with other business systems to achieve automated data management and applications.

Currently, the most commonly used environmental sensors include temperature and humidity sensors and pressure and chemical sensors for pollution monitoring.[1–3] These sensors are mostly based on wireless technology and are suitable for harsh conditions.[4–6] They are mainly based on chip technology and consist of integrated circuits, while the tags can derive energy

*Corresponding author: e-mail: wangbo_chen@126.com
https://doi.org/10.18494/SAM4676

ISSN 0914-4935

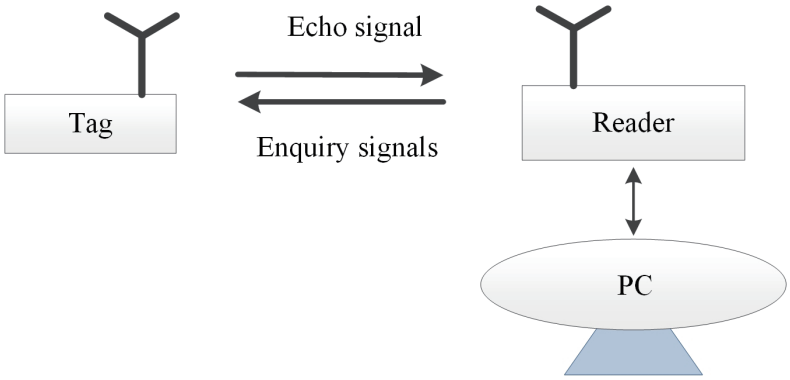

Fig. 1. RFID system workflow diagram.

from the integrated circuits. The presence of chips makes them unsuitable for various commercial applications owing to their relatively high price, and the overall cost of the system is affected by the RFID tags used. Thus, expensive tags end up making the system expensive, which triggers the need for designing low-cost chipless RFID tags.

Chipless RFID tags have attracted considerable attention from researchers owing to their advantages such as low cost and simple structure. Chipless RFID tags work on the principle of the backward scattering technique, where the reader emits an interrogation signal to the tag and then the tag reflects the encoded information to the reader.[7] Another module used along with RFID for IoT is the sensor. A sensor is a device used to detect and measure physical quantities or environmental parameters and is widely used in various fields such as IoT, intelligent control, monitoring data, medical devices, and the automotive industry. With the development and maturity of chipless RFID technology, the integration of sensors with chipless RFID technology is conducive to further realization of wireless sensing and the detection of physical parameters.

A tag based on a folded dipole resonator with a radar scattering cross section (RCS)[8] was designed to improve the coding capability of chipless tags by using different coding techniques. It was observed that the mentioned resonators were not able to achieve high bit density owing to their large size and reduced number of data bits used for encoding.[9] Capacitively loaded chipless RFID tag structures based on dipole resonators are reported in Ref. 9. Square-ring and crossed-ring resonator structures for chipless tags are also discussed. The reported structures are mainly designed to increase the bit density of the tags, but the overall bit density is estimated to be still low owing to their large dimensions of 17 × 68 mm^2 and 40 × 40 mm^2[10,11] and low bit capacity of 5 bits.[12] Therefore, they are considered unsuitable for data-intensive applications. In Ref. 13, a chipless tag based on a butterfly-shaped frequency selective surface with a 14 × 14 mm^2 footprint was implemented on a Rogers RT/droid/5880 substrate.[13] A 9-bit chipless tag structure consisting of circular grooves was designed, and its performance on flexible laminates was investigated. Another inverted m-shaped tag was designed as described in Ref. 14. These recently proposed chipless tags offer the best bit density, but they do not perform sensing. Therefore, they can only be used for identification without any additional services.[14]

In addition to identifying tags, smart RFID tags offer the benefit of ubiquitous sensing of various meteorological data, such as temperature and humidity. Chipless RFID sensor tags can utilize the loading of sensitive materials in the internal structure of the tag for the desired sensing purpose. To this end, diverse chipless tag designs have been reported in the literature, applying some sensitive materials such as paper.[15,16] In Ref. 16, a biodegradable paper substrate with dimensions of 44 × 59 × 0.54 mm^3 was used to fabricate RFID sensors, which had a read range of 4.57 m. In Ref. 17, a 16-bit extended c-shaped RFID sensor tag with silicon nanowires is proposed for sensing.[17] The size of the sensor is large (70 × 25 × 2 mm^3), so its manufacturing cost is high. In Ref. 18, a chipless wireless sensing sensor is introduced for humidity sensing by printing LC circuits on an FR4 substrate with a size of 85 × 53 mm^2, a humidity measurement range of 20 to 80%, and a sensitivity of 2.6 kHz/% RH when the distance between the reader and the sensor is 5 mm.[18] In addition, a 15-bit chipless tag with a size of 20 × 10 mm^2 was demonstrated, and the performance of humidity sensing was investigated to realize the concept of green electronics.[19] The aforementioned chipless tags use a paper substrate to sense humidity, which has several drawbacks. There is a strong relationship between the sensor parameters and the sensor response, which is nonlinear and ultimately affects the absorption peaks in the RCS curve when the paper is at high humidity levels. In addition, the paper may suffer from many structural deformation states and therefore compromise reliability.

The application of chipless RFID sensors in the field of intelligent packaging is the focus of research at this stage. Various perishable products (e.g., fruits and vegetables) must be kept fresh under certain humidity, temperature, and pH conditions,[20] and these types of sensor can be applied to these products. In 2020, Athauda *et al.* designed a chipless RFID pH sensor for smart packaging.[21] The sensor consists of four split rings, which are spaced from each other and can be considered capacitors, and for cheap pH sensing, these rings are covered with chitosan hydrogel. Experimental analyses showed that the chitosan hydrogel shows changes in frequency characteristics in both alkaline and acidic environments, which can be relied upon to determine the pH of the environment.

In this study, a humidity sensor consisting of an open-ring resonator and a U-shaped resonator as the sensor structure, Rogers TMM 4(TM) as the substrate, and a Kapton film as the sensitive material is designed. The sensor employs a backscattering technology to measure the humidity by covering the sensitive material on the resonator, where a change in humidity causes a change in the relative permittivity of the sensitive material, which in turn causes a change in RCS amplitude at the resonance point. The designed humidity sensor has the advantages of small size, high sensitivity, large measurement range, high operating frequency, and low production cost compared with other sensors.

2. Sensor Design

Microwave backscattering technology (MBT) is a wireless communication technology that is mainly used to achieve the automatic identification and tracking of objects. When a microwave signal is irradiated onto the surface of a target object, the irregular shape, texture, or material properties of the target object's surface will lead to the scattering phenomenon of the microwave

signal. The scattered signal is the signal scattered back by the microwave signal and has information related to the surface characteristics of the target object. By receiving and analyzing the microwave signal scattered back from the surface of the target object, some relevant information can be obtained. This information includes the intensity, phase, time delay, and other characteristics of the reflected signal. By processing this information, the state information of the target object can be inferred.

MBT is commonly used in radar, wireless sensor networks, and RFID applications. It can achieve noncontact, long-distance, real-time target detection and monitoring, and is widely used in object recognition, motion tracking, obstacle detection, and other fields.

2.1 Humidity sensor structure

The humidity sensor designed in this study consists of three parts, i.e., substrate, resonator, and sensitive material, and the shape of the sensor is schematically shown in Fig. 2.

Chipless RFID sensor substrates enable object identification and detection, as well as the acquisition of object-related environmental parameters through the integration of sensors and RF antennas. RFID substrates are often made of different materials to meet their different performance and manufacturing requirements, and the following are a few common RFID substrate materials: FR-4, Flexible Substrates, FR-1/FR-2, Rogers Series, and Metal Substrates. The sensor substrate material designed for this study is Rogers TMM 4(TM), with a relative permittivity of 4.5, a loss angle tangent of 0.002, and dimensions of 22 × 22 × 1.5 mm^3. This material has a low relative permittivity and a low dielectric loss, making it suitable for high-frequency and high-speed signal transmission applications. It has a wide range of applications in the RF, microwave, and millimeter wave fields such as satellite communications, radar systems, antenna design, and wireless communication equipment.

A resonator is a physical device or system capable of producing a resonant phenomenon at a specific frequency. When the external excitation frequency is close to or matches the intrinsic frequency of the resonator, the resonator can reach its maximum amplitude or response. The specific resonant frequency and performance characteristics of resonators make them an important component of electronic systems. The resonator designed in this study consists of a

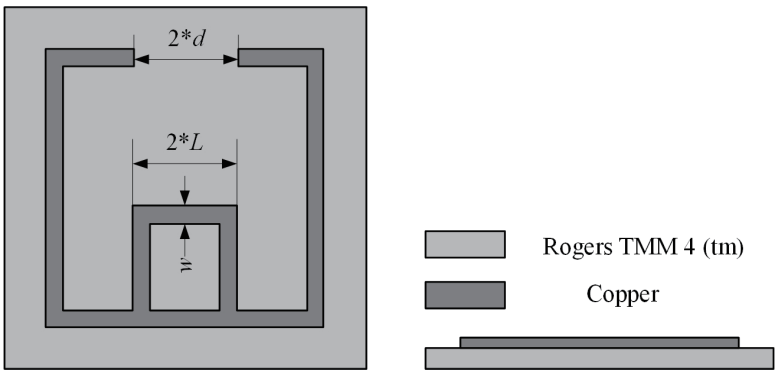

Fig. 2. Profile of humidity sensor structure.

square open-ring resonator and a nested U-shaped ring, as shown in Fig. 2. The overall dimensions of the resonator are 20 × 20 mm^2, where the outer edge of the square open ring is 20 mm long, the inner edge is 19 mm long, the width of the gap at the openings is set to be 2 × d, the width of the sides of the U-shaped ring is w, and the length of the outer edges is 2 × L. The design of the resonator in this study is based on the design of a square open-ring resonator and a U-shaped ring.

Sensitive materials are those that are sensitive to the external environment and can be measured, detected, or responded to. These materials typically exhibit observability or measurability about changes in the environment, such as changes in temperature, pressure, humidity, light, and chemicals. In this study, a humidity-sensitive material, Kapton film, is used, completely covering the resonator, with a size of 20 × 20 mm^2. It is a hydrophobic organic material with hydroxyl groups in its molecules, which absorbs water from the surrounding space. From the data on the dielectric properties of Kapton given in Ref. 22, the relative permittivity varies linearly with RH, which can be expressed as

$$\varepsilon_r = 3.05 + 0.008 \times \%RH \, . \tag{1}$$

2.2 Moisture-sensitive principle

Kapton is a high-performance polymer material with good thermal and chemical stabilities. When polyimide absorbs liquid or moisture, the adsorbed material enters the voids of the polyimide molecules or interacts with intermolecular forces, increasing the relative permittivity. In the absence of adsorbed substances, the relative permittivity of polyimide is usually low. However, when adsorbed substances enter the interior of a polyimide material, they occupy the intermolecular voids, increasing the polarization effect within the material and causing the electric field to interact with the adsorbed substances as it propagates through the material, thereby increasing the relative permittivity.

The detection parameter of MBT is mainly the radar scattering cross section (RCS). When using the RCS measurement, it is necessary to process the data through the spectrum to obtain the identified information, which can be detected in some more complex electromagnetic environments. In resonant circuits, the relative permittivity of the circuit elements will directly affect the resonant frequency and amplitude of the circuit. When the relative permittivity changes, the ability of the electric field to store and release energy in the capacitor also changes. Specifically, when the relative permittivity of a capacitor increases, it means that the electric field can be better stored and the capacitor's ability to respond to the electric field is enhanced, leading to an increase in RCS amplitude. Conversely, a decrease in relative permittivity leads to a decrease in RCS amplitude, which can be used to measure air humidity by linking relative humidity (RH) to the RCS amplitude through the relative permittivity.

3. Simulation Analysis

The structure shown in Fig. 2 is modeled in 3D using HFSS electromagnetic simulation software, and the simulation model is shown in Figs. 3(a) and 3(b).

(a) (b)

Fig. 3. (Color online) HFSS model of the sensor: (a) sensor model and (b) sensor in an air box.

When the overall dimensions of the sensor are fixed, the main factors affecting the performance of the whole sensor are the structural parameters of the resonator as well as air humidity, so when the structural parameters of the resonator are determined, air humidity can be analyzed. The control variable method is used to achieve optimization by adjusting three parameters, namely, the gap width d, the side width w, and the outer edge length L of the U-shaped ring. The relative permittivity of the Kapton film was set to 3.37, 3.45, 3.53, 3.61, 3.69, and 3.77, corresponding to RHs of 40, 50, 60, 70, 80, and 90%, respectively, to simulate the humidity change by changing its relative permittivity. The effects of gap width d, U-ring edge width w, and outer edge length L on the RCS amplitude are shown in Figs. 4(a)–4(e), 5(a)–5(e), and 6(a)–6(e), respectively.

It can be seen from Fig. 4(b) [same as Figs. 5(a) and 6(e)] that as the relative permittivity increases from 3.37 to 3.77 (i.e., RH increases from 40 to 90%), its RCS amplitude gradually increases, with the amplitude increasing by 7.52 dB from −65.66 to −58.14 dB, and thus the external ambient humidity can be measured.

Through a series of simulations, taking into account the RCS amplitude of the sensor as well as the resonant frequency, the following geometric parameters of the temperature sensor model proposed in this paper are determined: d = 1.1 mm, w = 0.1 mm, and L = 8.9 mm.

4. Results

Figure 7 demonstrates the variation between the relative permittivity and the RCS amplitude, and the relationship between RH and the relative permittivity is plotted through Eq. (1), as shown in Fig. 8. By relating the relative permittivity between Figs. 7 and 8, the relationship between RH and the RCS amplitude was obtained, as shown in Fig. 9.

As shown in Fig. 9, when the ambient humidity changes from 40 to 90%, the RCS amplitude increases from −65.66 to −58.14 dB, with an offset of 7.52 dB. The amplitude change is obvious, and the overall change is close to linear, with a sensitivity of 0.15 dB/%RH.

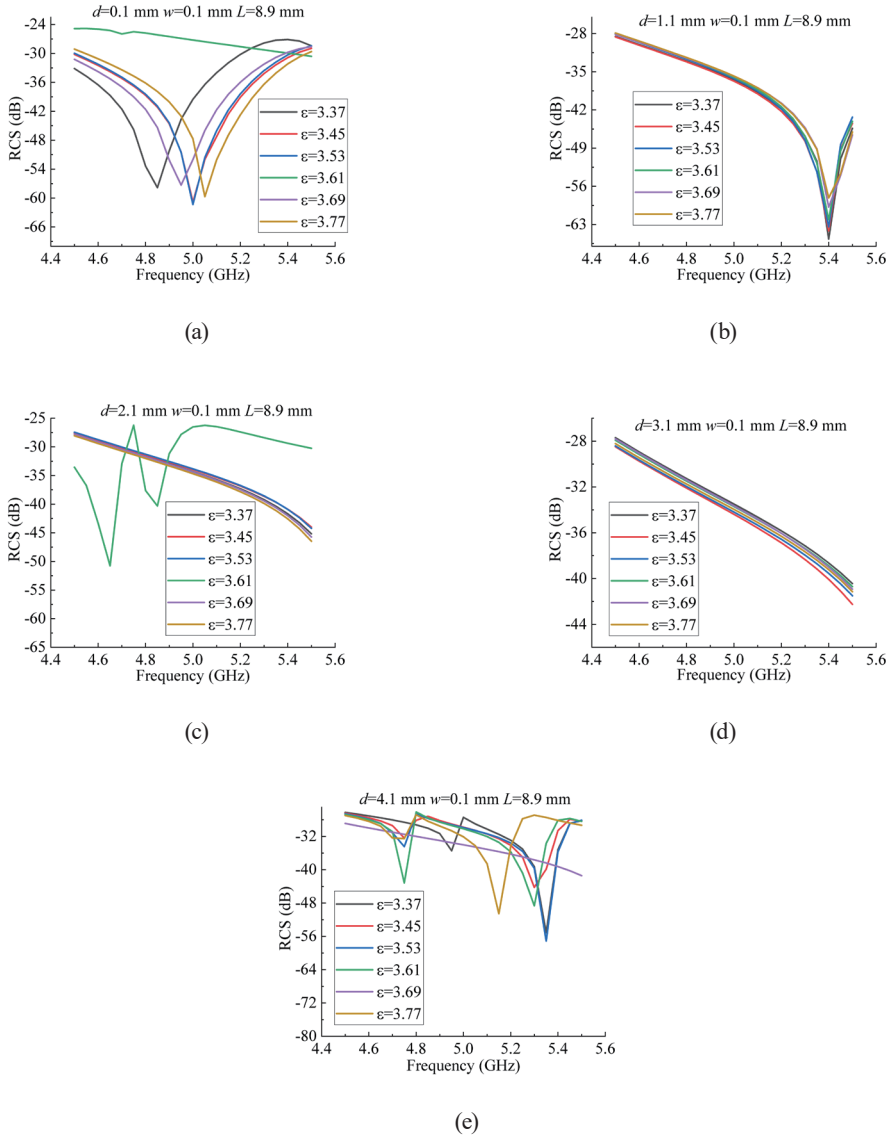

Fig. 4. (Color online) RCSs for different *d* values: (a) 0.1, (b) 1.1, (c) 2.1, (d) 3.1, and (e) 4.1 mm.

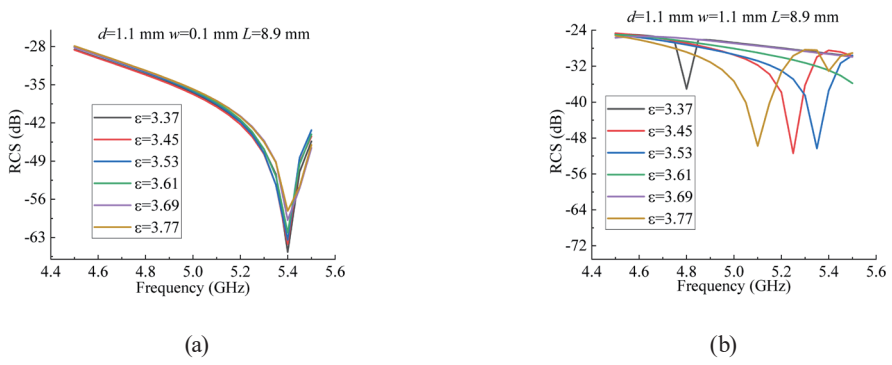

Fig. 5. (Color online) RCSs for different *w* values: (a) 0.1, (b) 1.1, (c) 2.1, (d) 3.1, and (e) 4.1 mm.

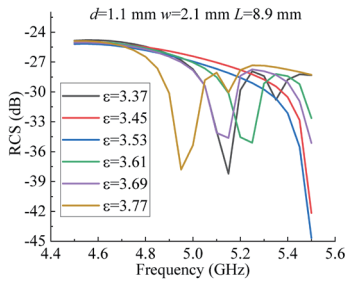

(c)

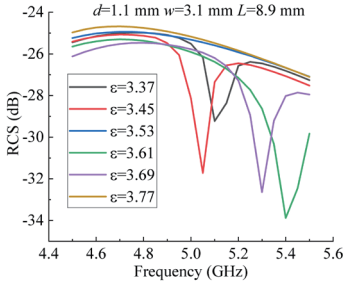

(d)

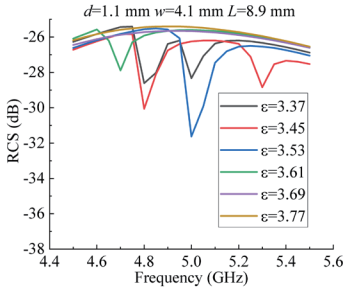

(e)

Fig. 5. (Continued) (Color online) RCSs for different w values: (a) 0.1, (b) 1.1, (c) 2.1, (d) 3.1, and (e) 4.1 mm.

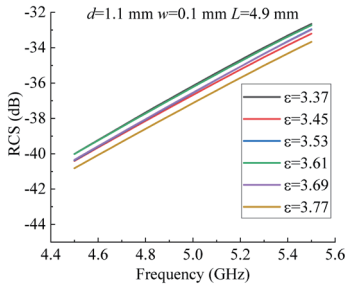

(a)

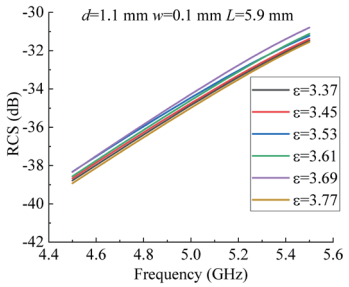

(b)

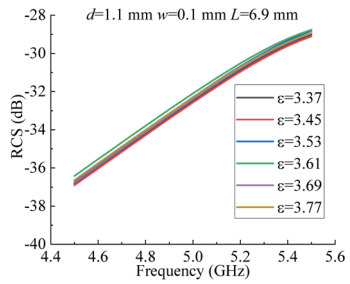

(c)

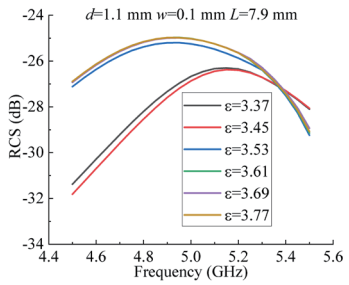

(d)

Fig. 6. (Color online) RCSs for different L values: (a) 4.9, (b) 5.9, (c) 6.9, (d) 7.9, and (e) 8.9 mm.

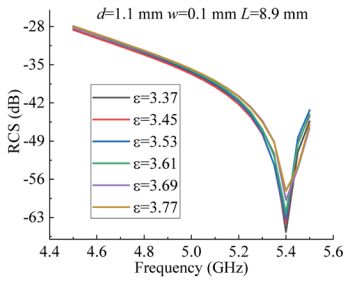

(e)

Fig. 6. (Continued) (Color online) RCSs for different L values: (a) 4.9, (b) 5.9, (c) 6.9, (d) 7.9, and (e) 8.9 mm.

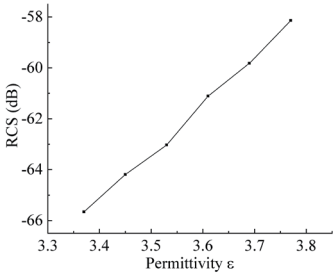

Fig. 7. Relative relative permittivity versus RCS amplitude.

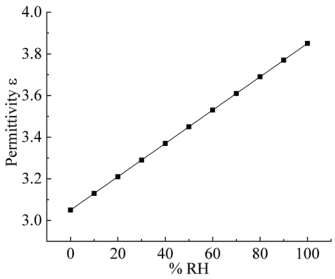

Fig. 8. Relative humidity versus relative permittivity.

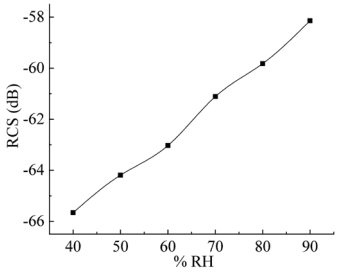

Fig. 9. Relative humidity versus RCS amplitude.

5. Conclusions

In this paper, a chipless RFID-based humidity sensor is proposed, which itself does not require an external power supply, and consists of a square open-ended ring combined with a nested U-shaped ring as the resonator structure, Rogers TMM 4(TM) as the substrate of the sensor, and a Kapton film as the sensitive material. In this study, we analyzed the effect of resonator size on the performance of the sensor and carried out HFSS simulation to simulate the

optimal resonator size in the frequency range of 4.5–5.5 GHz with a humidity measurement range of 40–90% and a sensitivity of 0.15 dB/% RH. The sensor designed in this study has the advantages of small size, low cost, high sensitivity, and large measurement range.

Acknowledgments

This research was funded by the Youth Science Foundation of the National Natural Science Foundation of China (No. 12204373) and the Natural Science Basic Research Program of Shaanxi (No. 2023-JC-QN-0002).

References

1 M. F. Farooqui, M. A. Karimi, K. N. Salama, and A. Shamim: Adv. Mater. Technol. **2** (2017) 1700051. https://doi.org/10.1002/admt.201700051
2 Y. Chen, Y. C. Wang, Y. Zhang, H. Zou, Z. Lin, G. Zhang, C. Zou, and Z. L. Wang: Adv. Energy Mater. **8** (2018) 1802159. https://doi.org/10.1002/aenm.201802159
3 Z. Duan, Y. Jiang, M. Yan, S. Wang, Z. Yuan, Zhen, Q. Zhao, P. Sun, G. Xie, X. Du, and H. Tai: ACS Appl. Mater. Interfaces **11** (2019) 21840. https://doi.org/10.1021/acsami.9b05709
4 Q. Tan, T. Luo, T. Wei, J. Liu, L. Lin, and J. Xiong: J. Microelectromech. Syst. **26** (2017) 351. https://doi.org/10.1109/JMEMS.2016.2642580
5 S. F. Shaikh and M. M. Hussain: Appl. Phys. Lett. 1**17** (2020) 074101. https://doi.org/10.1063/5.0017769
6 H. Kou, Q. Tan, Y. Wang, G. Zhang, S. Su, and J. Xiong: Sens. Actuators, B **311** (2020) 127907. https://doi.org/10.1016/j.snb.2020.127907
7 G. Khadka, M. S. Arefin, and N. C. Karmakar: IEEE Microwave Wireless Compon. Lett. **30** (2020) 701. https://doi.org/10.1109/LMWC.2020.2994189
8 O. Rance, R. Siragusa, P. Lemaitre-Auger, and E. Perret: IEEE Trans. Microwave Theory Tech. **64** (2016) 2315. https://doi.org/10.1109/TMTT.2016.2562625
9 J. Havlicek, M. Svanda, M. Polivka, J. Machac, and J. Kracek: IEEE Antennas Wirel. Propag. Lett. **16** (2017) 3051. https://doi.org/10.1109/LAWP.2017.2760059
10 N. Chen, Y. Shen, G. Dong, and S. Hu: IEEE Trans. Electron Devices **66** (2018) 200. https://doi.org/10.1109/TED.2018.2864623
11 F. Erman, E. Hanafi, E. H. Lim, W. A. Wan Mohd Mahyiddin, S. W. Harun, H. Umair, R.Soboh, and M. Z. H. Makmud: Electronics **8** (2019) 713. https://doi.org/10.3390/electronics8060713
12 V. R. Sajitha, C. M. Nijas, T. K. Roshna, K. Vasudevan, and P. Mohanan: Microwave Opt. Technol. Lett. **58** (2016) 944. https://doi.org/10.1002/mop.29706
13 M. A. Riaz, Y. Abdullah, H. Shahid, Y. Amin, A. Akram, and H. Tenhunen: Radioengineering **27** (2018) 776. https://doi.org/10.13164/re.2018.0776
14 W. M. Abdulkawi, A. F. A. Sheta, K. Issa, and S. A. Alshebeili: Electronics **8** (2019) 580. https://doi.org/10.3390/electronics8050580
15 S. Kim, A. Georgiadis, and M. M. Tentzeris: Sensors **18** (2018) 1958. https://doi.org/10.3390/s18061958
16 M. T. Islam, T. Alam, I. Yahya, and M. Cho. Sensors **18** (2018) 4212. https://doi.org/10.3390/s18124212
17 S. Genovesi, F. Costa, M. Borgese, A. F. Dicandia, G. Manara, S. Tedjini, and E. Perret: Proc. 2016 IEEE International Symposium on Antennas and Propagation (IEEE, 2016) 1275. https://doi.org/10.1109/APS.2016.7696345
18 J. F. Salmerón, A. Albrecht, S. Kaffah, M. Becherer, P. Lugli, and A. Rivadeneyra: Sensors **18** (2018) 2275. https://doi.org/10.3390/s18072275
19 S. Zeb, A. Habib, Y. Amin, H. Tenhunen, and J. Loo: Proc. 2018 IEEE Green Technologies Conf. (IEEE, 2018) 172-175. https://doi.org/10.1109/GreenTech.2018.00039
20 P. Fathi, N. C. Karmakar, M. Bhattacharya, and S. Bhattacharya: IEEE Sens. J. **20** (2020) 9618. https://doi.org/10.1109/JSEN.2020.2991751
21 T. Athauda, P. C. Banerjee, and N. C. Karmakar: IEEE Sens. J. **20** (2020) 8990. https://doi.org/10.1109/JSEN.2020.2986808
22 S. Habib, A. Ali, G. I. Kiani, W. Ayub, S. M. Abbas, and M. F. U. Butt: Int. J. Microwave Wireless Technol. **14** (2022) 176. https://doi.org/10.1017/S1759078721000362

About the Authors

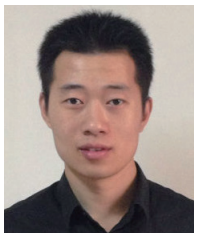

Bo Wang received his B.S. degree from Xi'an University of Technology of Xi'an, Shaanxi, China, in 2008. He received his M.S. and Ph.D. degrees from Xidian University, Xi'an, Shaanxi, China, in 2011 and 2016, respectively. He is currently a lecturer of Xi'an University of Posts and Telecommunications. His research interests include RFID systems, wireless sensor networks, and intelligent control. (wangbo_chen@126.com)

Junqiang He is a master's student at Xi'an University of Posts and Telecommunications, Xian, China. His recent research interests include RFID chipless tags and wireless sensor networks. (1843305196@stu.xupt.edu.cn)

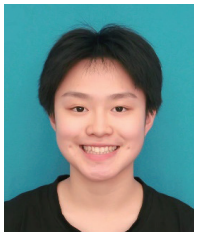

Yalun Song is an undergraduate student at Xi'an University of Posts and Telecommunications, Xian, China. Her recent research interests include RFID chipless tags and wireless sensor networks. (songyalun@stu.xupt.edu.cn)

Ke Wang graduated from the School of Mechano-Electronic Engineering of Xi'dian University in 2012 with a bachelor's degree. In 2021, she obtained a Ph.D. degree from Xi'dian University and then joined the School of Automation, Xi'an University of Posts and Telecommunications as an associate professor in the same year. Her research interests include the phononic and magnetic properties of two-dimensional materials. She has published many papers in Materials Horizons, Nanoscale, Physical Review B, Applied Physical Letters, and so forth. Her research interests include RFID chipless tags and wireless sensor networks.

Shengli Cao obtained Ph.D. degrees from Xi'an Jiaotong University and Tokushima University. He is an associate professor at the School of Automation of Xi'an University of Posts and Telecommunications. He has published over 20 high-level SCI papers and presided over one Natural Science Basic Research Program of Shaanxi. He is engaged in research based on nonlinear dynamics and fluid mechanics, and his main research content includes flow separation and control research under low Reynolds number conditions as well as Lagrange analysis methods.